Coherent Raman spectroscopy

Once exotic and time-consuming, wave-mixing spectroscopy has burgeoned into a set of techniques that can handle systems—flames, plasmas, luminescent crystals—inaccessible to conventional methods.

Marc D. Levenson

In 1928 Chandrasekhara Raman reported a process in which a material would simultaneously absorb one photon and emit another. The energies of the two photons differed by an amount corresponding to the energy difference between two quantum-mechanical levels of the medium. Raman scattering, as the phenomenon came to be known, provided a tool for the spectroscopic investigation of energy levels not accessible by the usual absorption and emission techniques. For the first thirty-five years Raman scattering was a laborious and exotic technique, important more for the quantum-mechanical principles it illustrated than for its practical applications.

Then, fifteen years ago, the development of gas lasers completely revolutionized the practice of Raman spectroscopy. Gone were the discharge lamps and hours-long photographic exposures; they were replaced by the cw laser, tandem monochromator and cooled photomultiplier. What had been a difficult and exotic technique became a routine analytical procedure for studying vibrational and other elementary excitations of materials.1 The development of powerful tunable lasers now promises a second revolution. Rather than randomly scattering photons as in present techniques, the Raman modes of a medium studied by coherent Raman techniques are made to emit a beam of coherent radiation containing the details of the spectrum. Samples in which the spontaneous Raman scattering is intrinsically weak, or masked by fluorescence and black-body radiation, can now be studied.

The advantages of the coherent Raman techniques result from the fact that the laser fields at two different frequencies can force a particular Raman mode of a medium to produce an oscillating dielectric constant which then interacts with one of the fields to produce a coherent output beam. The power in this beam can be many orders of magnitude larger than that in the spontaneously scattered radiation, and spatial filtering can be used to separate the output beam from unwanted radiation.

The essence of the process can be derived from a simple model. If we describe a Raman mode by a normal coordinate Q, then the first-order dependence of the polarizability α_{ij} of the medium upon Q is

$$\alpha_{ij} = \alpha^{0}_{ij} + \alpha'_{ij}Q \tag{1}$$

where i and i are two Cartesian coordinates and α' is just the conventional Raman susceptibility tensor. (In solids, the coordinate Q corresponds to a phonon with wavevector equal to the difference in wavevectors of the incident beams. For a polariton-a mode in a crystal lacking a center of inversion symmetry-the treatment is similar, but slightly more complex.) Because the electromagnetic free energy of such a medium contains a term proportional to QE^2 , there will be generalized force on the coordinate Q that is bilinear in the applied optical fields. If the equation of motion for Q is that of a damped harmonic oscillator with frequency ω_R , one can use Newton's second law to calculate the response to this

$$\begin{split} \ddot{Q} + 2\Gamma \dot{Q} + \omega_{\rm R}^2 Q \\ = \frac{1}{2} \left(N_1 - N_2 \right) \sum_{ij} \alpha'_{ij} E_i E_j \quad (2) \end{split}$$

As a concession to quantum mechanics I have included on the right a factor of N_1 — N_2 , giving the difference in the population of the two levels separated by the

Raman circular frequency ω_R .

If the electric field has frequency components at ω_1 and ω_2 , the force will have Fourier components at $\pm(\omega_1-\omega_2)$, which can drive the Raman mode resonantly when $|\omega_1-\omega_2|\approx\omega_R$. The oscillating coordinate then gives a modulated polarizability according to equation 1. An electric polarization $\mathcal P$ at the frequency $\omega_4=\omega_3\pm(\omega_1-\omega_2)$ results from the product of this oscillating polarizability and a Fourier component of the field at ω_3 : $\mathcal P_i(\omega_4)\propto$

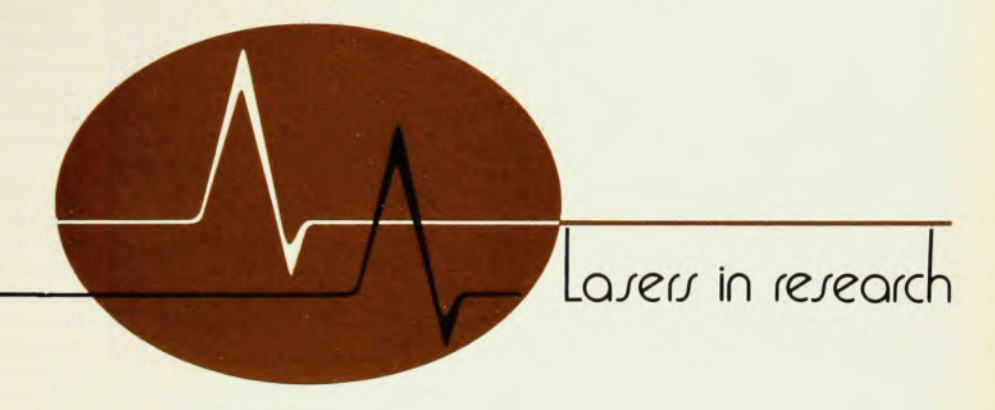
$$\sum_{jkl} \left[\frac{(N_1 - N_2)\alpha'_{ij}\alpha'_{kl}}{\omega_R^2 - (\omega_1 - \omega_2)^2 + 2i\Gamma(\omega_1 - \omega_2)} \right] \times E_i(\omega_3) E_k(\omega_1) E_l^*(\omega_2) \quad (3)$$

This polarization, which is cubic in the incident electric field amplitudes, acts as a source term in Maxwell's equation to produce² the output beam at ω_4 . The quantity in braces is sometimes termed the Raman contribution to the third-order nonlinear susceptibility, $\chi^{\rm R}_{ijkl}(-\omega_4, \omega_3, \omega_1, -\omega_2)$. If $N_2=0$, the overall four-photon parametric mixing process can be described by the level diagrams in figure

There are other processes involving molecular reorientation and real or virtual electronic transitions that also contribute to the radiated signal. These nonresonant background signals are pretty much independent of $\omega_1 - \omega_2$ and parametrized by another term in $\chi^{(3)}$ denoted χ^{nr}_{ijkl} . In some experiments the background level is interesting, in others merely a nuisance. The resonant Raman term interferes constructively and destructively with the background, producing a line-shape function with maxima and minima.

All the processes leading to output at ω_4 can be described by a third-order nonlinear susceptibility tensor $\chi^{(3)}_{ijkl}(-\omega_4, \omega_3, \omega_1, \omega_2)$. This is a fourth-rank tensor; of its four frequency arguments only three

Marc D. Levenson is an assistant professor of physics and electrical engineering at the University of Southern California, Los Angeles.



are independent because $\omega_1 + \omega_2 + \omega_3 \omega_4 = 0$. By convention the frequency arguments and polarization subscripts are paired and can be permuted as long as their pairing is respected.3 Symmetry considerations fortunately reduce the number of independent nonzero elements and permit classification of the symmetries of modes observed by coherent Raman techniques in different polarization conditions. Unlike the second-order nonlinear susceptibility responsible for optical second-harmonic generation, $\chi^{(3)}$ does not vanish identically for any symmetry group.2 Thus the techniques of coherent Raman spectroscopy are generally applicable.

One major advantage of these techniques is the large signal produced at ω_4 . The formalism of nonlinear optics can be used to estimate the power (in watts) radiated at this frequency as

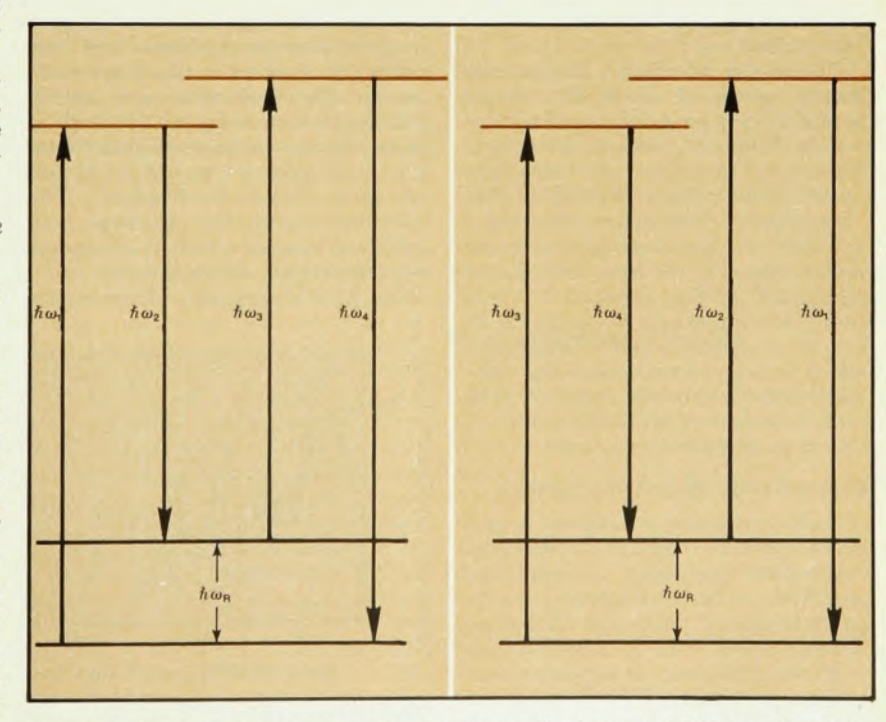
$$\begin{split} P_{i}(\omega_{4}) &= 2 \times 10^{-26} \, \frac{\omega_{4}^{2} \, l^{2} \mathrm{eff}}{n^{4} \, A^{2}} \, \bigg| \, \sum_{jkl} \chi^{(3)}_{ijkl} \, \bigg|^{2} \\ &\times P_{j}(\omega_{3}) P_{k}(\omega_{1}) P_{l}(\omega_{2}) \quad (4) \end{split}$$

Factors of order 4 resulting from frequency degeneracy have been suppressed in equation 4, and $P_i(\omega_1)$, $P_k(\omega_2)$, and $P_l(\omega_3)$ are the incident laser powers in watts at circular frequencies ω_1 , ω_2 and ω_3 polarized in the j, k and l directions, A is the area of the beams where they interact (in cm²), the linear index of refraction of the medium is n, and the nonlinear susceptibility $\chi^{(3)}$ is in electrostatic units. The effective interaction length (leff in equation 4) is always less than the distance over which the beams coincide. It depends in a rather complex way upon the wavevector mismatch of the interacting beams $\Delta k = |\mathbf{k}_1 - \mathbf{k}_2 + \mathbf{k}_3 - \mathbf{k}_4|$ and upon the details of the interaction geometry. Generally the best performance is obtained when Δk is as small as possible; if it is large, the interaction length scales as $1/\Delta k$. Negligible values of Δk occur automatically in several techniques of coherent Raman spectroscopy. In others, the propagation directions of the incident beams must be adjusted to approach optimum wavevector matching.

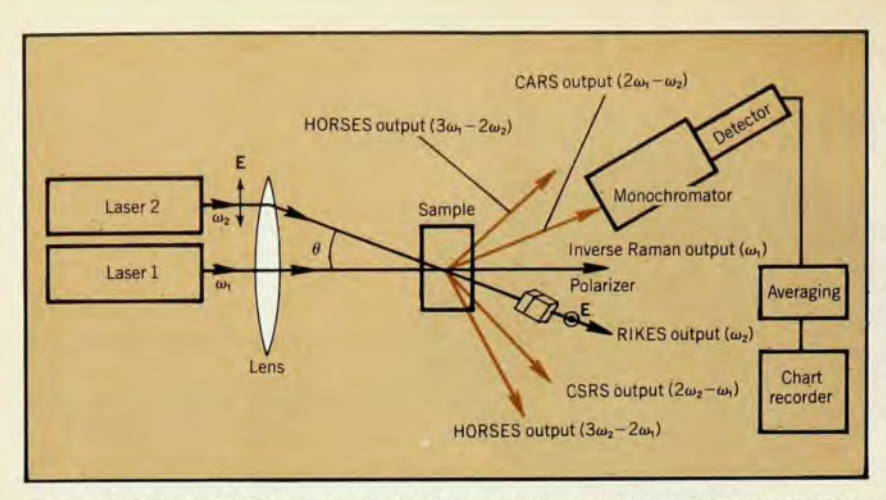
The radiated power depends upon the absolute square of the Raman susceptibility and upon the square of the interaction length. For typical liquids and solids, these parameters have values of about 10^{-13} esu and 0.1 cm, while at

standard temperature and pressure, typical gases have nonlinear susceptibilities 100 times smaller but permit interaction lengths 10 times longer. In a coherent Raman experiment in which 10-kW lasers are focussed into an area of 10^{-5} cm², equation 4 gives an output of 0.055 W for $\chi^{(3)}=10^{-13}$ esu and $l_{\rm eff}=0.1$ cm, and 0.002 W for $\chi^{(3)}=10^{-15}$ esu and $l_{\rm eff}=2$ cm, for output at 5000 Å.

The data-collection rate, however, is proportional to the rms output power. For lasers pulses 6 nanosec long and a



Typical level diagrams for coherent Raman processes. Physical optical fields must have both positive- and negative-frequency components, but the detected frequency must correspond to some sum of the inputs. The diagram on the left shows four-photon parametric mixing of the "CARS" type, and that on the left, a process of the "RIKES" type.



The layout of a typical CARS experiment, also showing the directions of the output beams for some other coherent Raman techniques: RIKES, CSRS, HORSES and the inverse Raman effect. In four-wave mixing an additional beam would be added, collinear with that from laser 1. The RIKES output has its electric-field vector polarized normal to the beam.

repetition rate of 15 pulses per sec, the rms output is 16.5 microwatts for a "typical" solid, and 0.6 microwatt for a "typical" gas. In a spontaneous scattering experiment in which 10^7 photons at 5000 Å are collected per second, the rms signal power is 4×10^{-12} W.

According to equation 4, the rms output power is proportional to the time average of a cubic product of laser powers. Taken literally, this implies that large, slowly firing pulsed lasers will give the best performance. In practice, modest pulsed lasers that have high repetition rates are more convenient. Excellent results have been obtained with cw lasers, especially when the sample can be inserted into the laser cavity.

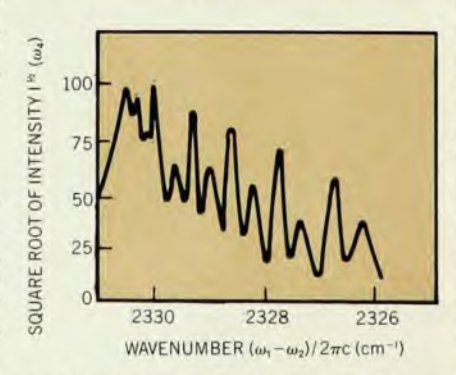
The several advantages of observing Raman spectra by means of nonlinear optical mixing have been realized in a variety of coherent Raman spectroscopic techniques. Acronyms and neologisms such as CARS, RIKES, HORSES, CSRS, "Submarine," "Helicopter," "Asterisk," and so on have been invented to designate each variation of the basic four-photon parametric mixing process.4-7 spectroscopic tool each technique has its own set of advantages and disadvantages, and it is important to match the technique properly to the investigation. The main alternatives are individually reviewed in the following sections.

Coherent anti-Stokes Raman spectra

In the most widely practiced technique of coherent Raman spectroscopy, two incident laser frequencies are employed, and $\omega_3 = \omega_1$ in the level diagram shown in part a of figure 1. The output frequency is then $\omega_4 = 2\omega_1 - \omega_2$. If ω_1 corresponds to the laser frequency in a spontaneous-scattering experiment and ω_2 to the Stokes-scattered photon, the output occurs at the corresponding anti-Stokes frequency. (If ω_1 is less than ω_2 , the analogous technique is called Coherent

Spectroscopy Stokes Raman or CSRS-pronounced "scissors.") Paul Maker and Robert Terhune, using discrete frequencies, initially demonstrated this technique in 1965.3 It did not become a practical spectroscopic tool until 1972, when several groups began to employ repetitively pulsed dye lasers for continuous scanning of the Raman spectrum.11,12 An excellent review article recounts many of the recent results obtained using this technique, so there is no need for more than an overview here.8

Figure 2 depicts a typical CARS experimental setup, along with the outputs used in other coherent Raman techniques. Two lasers are focussed into a sample with an angle between the beams that best fulfills the wavevector-matching condition for the overall three-wave mixing process: $\Delta k = 0$. In gases this angle is essentially zero, but in condensed phases it depends upon $\omega_1 - \omega_2$ and the dispersion of the index of refraction. The beam that emerges from the sample at ω_4 is selected by means of filters or a simple monochromator, and its intensity is detected photoelectrically. To scan, the



The Q branch of nitrogen at atmospheric pressure as it appears in a CARS trace. The ordinate is the square root of the intensity at $2\omega_1-\omega_2$, which is roughly linear in the Raman scattering cross section. Figure 3

difference frequency $\omega_1 - \omega_2$ is varied by tuning one or both lasers. Plotted as a function of $\omega_1 - \omega_2$, the output reflects the Raman spectrum of the sample.

The tremendous power of this technique for taking Raman spectra of gases can be illustrated by a few examples. With laser powers of 2 MW at ω_1 and 0.2 MW at ω_2 , and $\omega_1 - \omega_2$ at the Q branch of the breathing-mode ($v_1 = 0 \rightarrow 1$) transition in methane, Albert Harvey and Joseph Nibler found that the CARS output beam from a 0.1-Torr sample was strong enough to be seen by eye. Similar lasers 1000 times stronger are already being used in studies related to isotope separation. Conservatively, an improvement in sensitivity of three orders of magnitude can be expected when these more powerful lasers are used for CARS.

In an ingenious experiment with cw lasers, A. Hirth and K. Vollrath obtained the Q-branch spectrum of atmospheric pressure nitrogen that appears in figure 3-in ten milliseconds! Conventional scattering techniques would take nearly an hour to give a comparable resolution and signal-to-noise ratio. Even more rapid data collection is possible when the intensity is measured simultaneously in many separate frequency channels. That can be done conveniently by making laser 2 in figure 2 oscillate over a band of The various frequency frequencies. components of the output beam can then be separated with a spectrometer and recorded simultaneously on a multichannel detector such as a photographic plate, optical multichannel analyzer or vidice a camera. Won Roh, Paul Schreiber and Jean-Pierre Taran employed such a system to resolve the Q branch of the vibration quantum number $v = 0 \rightarrow 1$ transition in H2 with a single 20-nsec laser pulse. Rapidly evolving systems such as explosions and shocks can obviously be studied by this technique if the lasers are properly synchronized.

Wolfgang Kaiser and A. Laubareau have used synchronized picosecond lasers in CARS-related experiments to measure the dephasing and decay times of phonons and of nolecular vibrations. In these experiments, a delayed pulse at ω1 samples the amplitude of the oscillation previously excited by simultaneous pulses at ω_1 and ω_2 . The decrease in coherent anti-Stokes intensity with increasing delay time gives the dephasing, while the decrease in spontaneously scattered anti-Stokes radiation parametrizes the decay. Relaxation times of one or two picoseconds can be measured with good accuracy, and some questions related to the mechanisms for broadening of Raman lines can be answered.10

Some other virtues of the CARS tech-

nique deserve mention.

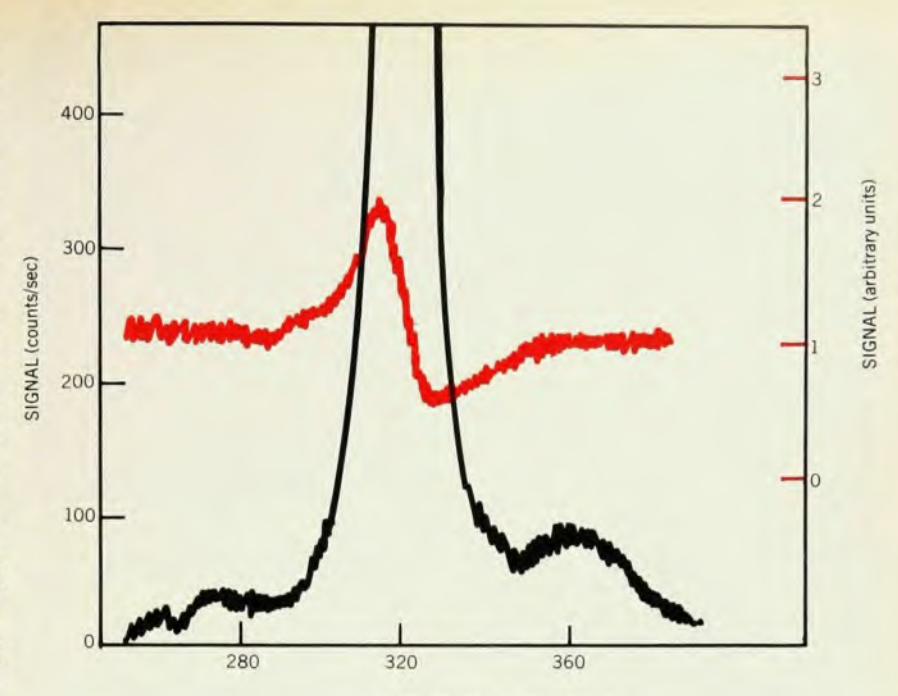
▶ The CARS technique has considerable potential for precision spectroscopy. The resolution of these experiments is limited by the laser linewidth, which can be readily reduced to 15 MHz and perhaps below. Inhomogeneous broadening due to the Doppler effect contributes a width of $\omega_R[(kT/2mc^2)\ln\ 2]^{1/2}$ where m is the mass of the molecule and all beams are collinear. That means that precision measurements of rotational and vibrational Raman frequencies can now be made precise enough to elucidate the structure of molecules lacking microwave absorption bands.

The intensity of coherent anti-Stokes radiation emitted from a region of an inhomogeneous sample is related to the local concentration of the Raman active material. This fact has been exploited to produce images showing the distribution of substances in a flame or jet, and it might be applicable to living cells. 11

Figure 4 illustrates one difficulty in applying CARS technology to solids, liquids and solutions. In that figure, the colored curve is the CARS spectrum of calcium fluoride in the region of the relatively weak 320 cm⁻¹ mode. That mode appears as a slight variation in the level of a signal dominated by a nonresonant background due to virtual electronic transitions.12 For comparison, the black curve shows the spectrum obtained with up-to-date spontaneous scattering technology!13 An analysis of the line shape in the CARS spectrum reveals the ratio of the peak Raman contribution to the nonresonant background term. nonresonant third-order susceptibility is of some interest in nonlinear optics, and because the Raman term can be related to well determined spontaneous-scattering cross sections, this technique gives accurate measurements of this quantity. However, to see weak spectroscopically interesting modes by coherent techniques it is necessary to suppress the nonresonant background. Without such suppression, the coherent Raman techniques are actually less effective than spontaneous scattering in detecting Raman spectra of condensed phases.

Raman-induced Kerr effect (RIKES)

The simplest method promising background suppression employs the Raman-induced Kerr effect proposed originally by Robert Hellwarth.5 This phenomenon results from a source polarization of the form given in equation 4, but with $\omega_3 = -\omega_1$; its level diagram is shown in part b of figure 1. The wave that results from the coherently driven vibration is at the same frequency as one of the inputs (that is, $\omega_4 = -\omega_2$) but polarization selection rules are employed to ensure that the radiated field is in a different state of polarization than the input laser. Essentially, the driven vibration produces an intensity- and frequencydependent birefringence, which alters the polarization condition of a wave probing the sample. The wavevector-matching condition is automatically fulfilled, and if the ω1 beam is circularly polarized, the



WAVENUMBER Δω/2πc (cm⁻¹)

Two traces of a phonon mode in calcium fluoride. The colored line is a CARS trace; the black line is the same 320-cm⁻¹ mode, as resolved with spontaneous scattering and pulsed lasers. The vertical scales have been adjusted to give about equal noise levels.

nonresonant background is eliminated.

The early RIKES experiments employed a linearly polarized probe beam at ω_2 and a circularly polarized pump at ω_1 . After the sample, a crossed polarization analyzer blocked the probe intensity except when $|\omega_1 - \omega_2| = \omega_R$, in which case a small transmission was detected. The overall experimental scheme was otherwise quite similar to figure 2. Slight birefringence due to strains in the sample or optics led to a small background transmission of the probe frequency even when the pump beam was blocked.

This background, however, could be used to enhance the sensitivity of the technique. The field radiated as the result of the coherent Raman process interferes constructively or destructively with the background, producing an enhanced change in transmitted intensity. If the pump laser is then modulated, electronic techniques can detect the quite small modulations in the transmitted intensity caused by the coherent Raman process. Background-free Raman spectra are obtained with a sensitivity limited only by the fluctuations in the probe-laser intensity. This technique also can be used to separately determine the real and imaginary parts of the complex nonlinear polarization in equation 3 as well as the real and imaginary parts of the total nonlinear susceptibility tensor. differential cross section due to spontaneous Raman scattering is proportional to the imaginary part of this susceptibility, and so spectra taken with this technique can have a familiar appearance. The signal also scales linearly with density and cross section, facilitating the identification of modes by their relative intensities.

Spectra similar to figure 4 appear when a pump is employed linearly polarized at an angle to the polarization of the probe. Analysis of the resulting line shape relates the Raman cross section, optical Kerr constant and other terms in $\chi^{(3)}$ to one another. RIKES also has advantages for studying low-frequency modes. When $\omega_1 - \omega_2$ approaches zero, the CARS wave-vector-matching condition requires collinear propagation, making separation of the signal beam difficult. No such geometrical restriction applies to RIKES, and polarization selection and spatial filtering easily extract the signal.

Four-wave mixing techniques

Providing a third input frequency adds valuable extra degrees of freedom to CARS and RIKES experiments. If the detected frequency is at $\omega_4 = \omega_1 + \omega_3 - \omega_2$, Raman resonances occur when $|\omega_1 - \omega_2|$ = ω_R and when $|\omega_3 - \omega_2| = \omega_R$. The line shapes observed when the two different frequencies excite different Raman modes determines the ratio of the Raman cross sections. Alternatively, $\omega_3 - \omega_2$ can be set to a frequency at which the Raman contribution from one mode nearly cancels the nonresonant background. The sensitivity with which Raman modes are detected near $\omega_1 - \omega_2$ is markedly increased.14

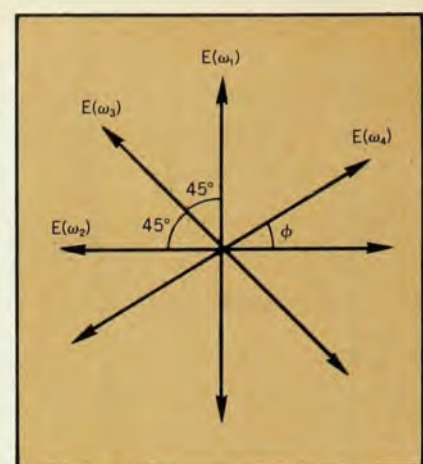
Nonresonant background signals can be completely eliminated with four-wave

mixing in certain polarization configurations. The most flexible of these is the "Asterisk" configuration shown in figure 5, which works for the four-wave analogs of CARS ($\omega_4 = \omega_1 + \omega_3 - \omega_2$) and of RIKES ($\omega_4 = \omega_2 - \omega_1 + \omega_3$).⁷ The planes of polarization of the input waves at ω_1, ω_2 and ω_3 are at 45° to one another, while a polarization analyzer selects the component of the output at the angle ϕ . For some particular value of ϕ -generally near 45°-the background level will vanish. With the background gone, photons appear at frequency ω4 only when a Raman resonance condition exists. Weak Raman modes can be detected with a sensitivity limited only by the quantum nature of light. The difference between CARS and Asterisk spectra is demonstrated in figure 6.

The strength of the observed intensity depends quadratically upon the Raman cross section and the concentration, and on the product of the intensities of the three lasers. The present practical limit in liquid solution corresponds to the detection of a 0.03-molar solution of benzene in a Raman-inactive solvent. That may be enough sensitivity to study biologically interesting materials in dilute solution if the Raman tensor is enhanced by pre-resonance phenomena. With stronger lasers lower concentrations and weaker modes can be investigated.

Other techniques and applications

Gain and loss due to the stimulated Raman effect can also be used for spectroscopic purposes.¹⁵ These phenomena are described by a polârization of the form in equation 3 with $\omega_3 = -\omega_1$ and $\omega_4 = -\omega_2$



The "asterisk" polarization condition. All the input waves are plane polarized as shown; an analyzer selects the desired component of the output wave.

Figure 5

as in RIKES, but no polarization selection is necessary. An input laser at ω_2 will be amplified by the Raman interaction if $\omega_1 - \omega_2 \approx \omega_R$ in the stimulated Raman effect, and attenuated if $\omega_2 - \omega_1 \approx \omega_R$ by the so-called "inverse Raman effect." With enough intensity at ω_1 , large signals at the Stokes frequency can be built up from noise and large anti-Stokes intensities can be completely absorbed. These techniques enjoyed considerable interest at one time, but enthusiasm waned when it became apparent that only the strongest Raman modes produced measurable differences in the intensity at ω_2 .

Improved technology—especially the

to determine the absolute scattering cross section. Changes in laser intensity of one part in 105 due to the stimulated Raman effect are detectable. This is less sensitivity than the optical mixing techniques can muster, but more than enough for accurate measurement of nonlinear optical parameters and Raman cross sections. When the output beam of an optical mixing experiment becomes strong enough, it too can mix with one of the incident fields to drive a vibration and create a new output frequency. In this way coherent second Stokes and second anti-Stokes beams have been generated in the imaginatively named Higher Order Raman Spectral Excitation Studies (HORSES), which oddly enough were

development of stable cw dye lasers and

the application of interferometric tech-

niques to nonlinear spectroscopy-has

revived interest in these methods. Using

a Jamin interferometer, Adelbert

Owyoung has measured the Raman amplification and intensity-dependent dis-

persion due to 992-cm⁻¹ mode of benzene

The technology of coherent Raman spectroscopy can also be used to study other kinds of transitions. One- and two-photon absorption processes lead to resonances in the "nonresonant" contribution to the third-order nonlinear susceptibility and result in observable variations in the output-wave intensity.²

demonstrated after CARS.6 These extra

frequency components may prove useful

in doing Raman spectra of absorbing

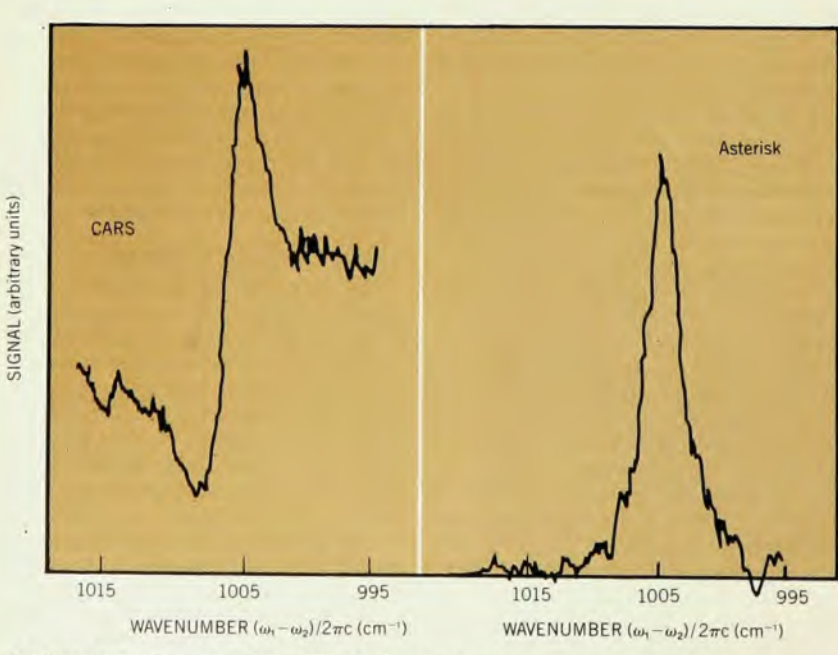
samples.

Steven Kramer and Nicolaas Bloembergen have used such a two-photon resonance to probe the Z₃ exciton in CuCl. 16 The homogeneous linewidth of an inhomogeneously broadened one-photon transition can be estimated from the linewidth of the CARS "Rayleigh resonance" observed when $\omega_1 - \omega_2 \rightarrow 0$ in an absorbing material. The analogous RIKES experiment is a variation of the "polarization spectroscopy" technique reviewed on page 34 in this issue of PHYSICS TODAY by Theodor Hänsch. Tatsuo Yajima has pointed out that a detailed analysis of the line shape of the Rayleigh resonance permits estimation of both the longitudinal and transverse relaxation times for an inhomogeneously broadened two-level system.17

When to use these techniques?

Coherent Raman spectroscopy today provides a valuable supplement to the conventional technique of spontaneous scattering. But the techniques are all rather cumbersome, relying on newly developed technology, while the apparatus necessary for scattering has benefited from fifteen years and more of engineering development. When is the extra effort—and extra expense—worthwhile?

At present, if an investigation can be



CARS and asterisk spectra of the 1005-cm⁻¹ mode of sodium benzoate in a ½-molar water solution. The nonresonant background due to the solvent has been suppressed in the asterisk spectrum by a factor of more than a thousand, enhancing the detection sensitivity.

performed by using spontaneous scattering with modest lasers, it should be done in that way. Certain systems—low-pressure gases, flames, plasmas, luminescent molecules and crystals-can not be easily studied by scattering. Again, certain parameters-nonlinear susceptibility tensor elements, dephasing and decay times, rotational constantscan not be measured with sufficient precision, if at all. These must be investigated by coherent techniques.

As time goes on, coherent Raman spectroscopy will become more convenient and less expensive, and the difficult tasks reserved for coherent Raman spectroscopy will become more routine. Continued technological innovation may ultimately make the coherent Raman techniques as accessible as spontaneous

scattering is today.

This work has been supported by the National Science Foundation and the Alfred P. Sloan Foundation.

References

- 1. M. C. Tobin, Laser Raman Spectroscopy, Wiley, New York (1971); T. R. Gilson, P. J. Hedra, Laser Raman Spectroscopy, Wiley, New York (1970).
- 2. C. Flytzanis, in Quantum Electronics, volume 1A (H. Rabin, C. Tang, eds.), Academic, New York (1975); C. Flytzanis, N. Bloembergen, in Progress in Quantum Electronics (J. H. Sanders, S. Stenholm, eds.), volume 4, part 3, Pergamon, New York (1976).
- 3. P. D. Maker, R. W. Terhune, Phys. Rev. A 137, 801 (1965).
- 4. R. F. Begley, A. B. Harvey, R. L. Byer, Appl. Phys. Lett. 25, 387 (1975).
- 5. D. Heiman, R. W. Hellwarth, M. D. Levenson, G. Martin, Phys. Rev. Lett. 36, 189 (1976).
- 6. I. Chabay, G. K. Klauminger, B. S. Hudson, Appl. Phys. Lett. 28, 27 (1975).
- 7. J. J. Song, G. L. Eesley, M. D. Levenson, Appl. Phys. Lett. 29, 567 (1976).
- 8. W. M. Tolles, J. W. Nibler, J. R. McDonald, A. G. Harvey, Appl. Spectroscopy 31, 96 (1977).
- 9. A. B. Harvey, J. R. McDonald, W. M. Tolles, in Progress in Analytical Chemistry, Plenum, New York (1977).
- 10. W. Kaiser, A. Laubareau, in Tunable Lasers and Applications (A. Mooradian, I. T. Jaeger, P. Stoketh, eds.), volume 3, Springer, New York (1976), page 207.
- 11. P. R. Regnier, in Laser Raman Gas Diagnostics, (M. Lapp, C. M. Penney, eds.) Plenum, New York (1974).
- 12. M. D. Levenson, N. Bloembergen, Phys. Rev. B 10, 4447 (1974).
- 13. P. Yaney, J. Raman Spectroscopy 5 (to be published).
- 14. H. Lotem, R. T. Lynch Jr, N. Bloembergen, Phys. Rev. A 14, 1748 (1976). 15. W. T. Jones, B. P. Stoicheff, Phys. Rev.
- Lett. 13, 657 (1964). 16. S. D. Kramer, N. Bloembergen, Phys. Rev.
- B 14, 4654 (1976). 17. T. Yajima, Opt. Comm. 14, 378 (1975).

Indestructible Mirrors?



If high damage threshold and low distortion are two of your concerns, write for our 23-page technical report, "Metal Mirror Selection Guide". It will give you the latest data on metal mirror performance characteristics, and help you choose the mirror that's right for your application.

Spawr Optical Research is the major supplier of state-of-the-art metal mirrors to researchers throughout the world.

SPAWR OPTICAL RESEARCH, INC. 1521 Pomona Road, Corona, Ca. 91720 714/735-0433